

The Effect of Basis Mass on Metronome Synchronization

Filippos Fotiadis, Aris Kanellopoulos, Nick-Marios T. Kokolakis

Abstract

In this project, we study the effect of the mass of a platform on the coupling and the synchronization of an array of metronomes. In particular, we develop a MATLAB code that takes as its input a video and outputs the angle of the metronomes, by utilizing color-coded pointers. Next, we incrementally increase the mass of the platform on which the metronomes are placed, and we investigate how the time to synchronization varies as this mass changes. We compare our results to theoretical models in a quantitative way.

I. INTRODUCTION

Over the course of the last four centuries, there have been extensive studies regarding synchronization phenomena, owing to their relevance to a huge variety of fields [1]. Synchronization was initially investigated in the mechanical domain in 1657, by the physicist Christiaan Huygens. In particular, while being at his laboratory, Huygens noticed that synchronization was happening between two pendulums, which were hanging by an overhead beam. Huygens initially explained this phenomenon wrongfully; he thought that the synchronization was the result of air fluctuation forced by the oscillations of the two pendulums. Nevertheless, he carried out experiments which allowed him to describe the stability and time properties of his pendulum system, even though he was unable to do this with mathematical rigorosity [2].

The importance of researching synchronization can be understood by looking at the variety of different fields where synchronization models have been adopted. Perhaps the most significant applications of synchronization can be found in modeling biological phenomena [3]. The synchronization of firefly light emission [4] is one such phenomenon, where individual fireflies sparkle with frequencies and phases that tend to be aligned. Another biological example can be found in the electric patterns of the brain. In particular, Norbert Wiener, who studied human brain waves, noticed a rise of activity in electroencephalograms over a small spectrum of frequencies close to 10Hz. As a result, he made the hypothesis that oscillating brain elements followed a coupled behaviour that leads to this frequency locking [5]. Even though Wiener did not wrap up his findings to create a theoretic model, researchers in the subsequent years discovered the mechanism that makes neurons synchronize their spiking behavior. In fact, they concluded this synchronization results in the creation of macroscopic capabilities in the brain, such as memory storing [6].

As one would expect, the phenomenon of synchronization is not confined to biological systems, but has been observed and exploited in a variety of areas [7]. Rather not unexpectedly, one such area where synchronization phenomena take place is social sciences. Owing to the effect that personal opinions of individual agents have on their surroundings, the resulting collective behavior of rational agents has been studied from a synchronization-theoretic perspective. In particular, the authors in [8] created a Kuramoto-based model of opinion-dynamics that is vastly different from the conventional consensus-based ones.

A wide range of engineered systems has been designed according to the principles of synchronization. Data-mining algorithms have been crafted, which transform encoded data vectors, retrieved from a source of raw data, into vectors of natural frequencies for the dynamical model of an oscillator. The notion is that algorithms simulating synchronization dynamics will partition similar data into clusters, hence discovering patterns in data sets [9]. In a similar manner, the production, dissipation, transformation, and consumption of power by a power grid is equivalent to a dynamical problem; the power grid can be thought of as a system of oscillators, which follow the second order Kuramoto model [10].

Although the synchronization of mechanical oscillators was the first to be studied, it still constitutes an important research topic up to today. In order to conduct a deeper investigation of the underlying mechanisms and to improve our understanding of the emergent behaviors, efforts have been concentrated on the experimental study of metronome synchronization. Metronomes have been used as a means to imitate the pendulum clocks of Huygens in a less sophisticated way. Pantaleone [11] constructed a theoretical model to describe the synchronization mechanism of metronomes, which are interconnected with one another through a base that can only move in one direction. He also showcased how his derived equations could lead to a Kuramoto model of the procedure, a famous theoretical system employed in order to capture the phase dynamics of interconnected oscillators [12].

The model that was created by Pantaleone has been studied in an extensive manner. Various studies [13] have examined the nature of steady state frequency synchronization; they have concluded that as the number of metronomes increases, many different equilibria are generated. For example, when phase locking takes place, the metronomes share the same phase in their oscillations. On the other hand, with anti-phase locking, the system of the metronomes converges to a state where there are two groups of oscillators, which have a phase difference of π . The phenomenon of chimera may also take place, which causes a part of the oscillators to synchronize and another part to oscillate incoherently [14]. Furthermore, coupled mechanical oscillators have been studied with regards to other of their properties. In particular, the authors of [15] recently carried out a stability analysis for the synchronization of a system of two pendulums. This is very representing of the interest of the scientific community on the analysis of the metronome system. In [16], the authors investigated the impact of different metronome lengths on synchronization, while the authors in [17] analyzed the behavior of two metronomes by changing the rolling friction of a PVC rolling basis, and presented the corresponding bifurcation diagrams.

Following these research directions, in this project we will focus on the robustness, stability and convergence properties of a dynamical system of three coupled metronomes manifesting phase locking, and the effect that variations in the mass of the platform has on the aforementioned properties. To this end, we set up a widely-used structure of metronomes operating on a common platform, itself resting on two soda cans. The mass of the platform was altered by the addition of weights in equal discrete steps, while visual measurements from a camera allowed us to derive the trajectories of the metronomes.

II. EXPERIMENTAL SETUP

We will now describe the setup that we used for the experiments carried out in this project. The principal component of the setup were the metronome oscillators, the number of which was restricted to three. There are several studies that use even double or triple of this number of oscillators, but our choice to use only three came down to two reasons. First, a large quantity of metronomes complicates the measurement process, because the camera that films them needs to be further away from them. Second, we have noticed that the more quantitative experiments restrict the number of metronomes to just three. We used metronomes of the brand Wittner, whose frequencies were preset to 184 beat (half-oscillations) per minute. That would be equivalent to oscillations with a period of $T = 0.652s$. The metronomes have virtually no energy loss, as they replenish it through their hand-wound spring; more details regarding this energy will be provided later on.

The interconnection between the metronomes was attained by placing them on a board, which consists of an orthogonal piece of rigid material. The fact that the board is rigid is very important, as it results in virtually lossless transmission of inertial forces among the oscillators. To keep the weight of the board at relatively low levels, we chose to use a foam or a tin base. The coupling between the metronomes also relies on placing the rigid board on two soda cans. These are also rigid in order to minimize deformation as well as the friction between them and the board, as we will notice in the following sections. In addition, the soda cans can only move in one direction. Finally, in order to study the sensitivity of the synchronization of the metronomes with respect to the mass of the platform, we incrementally increased the mass of the rigid board by placing additional weights on it. These weights

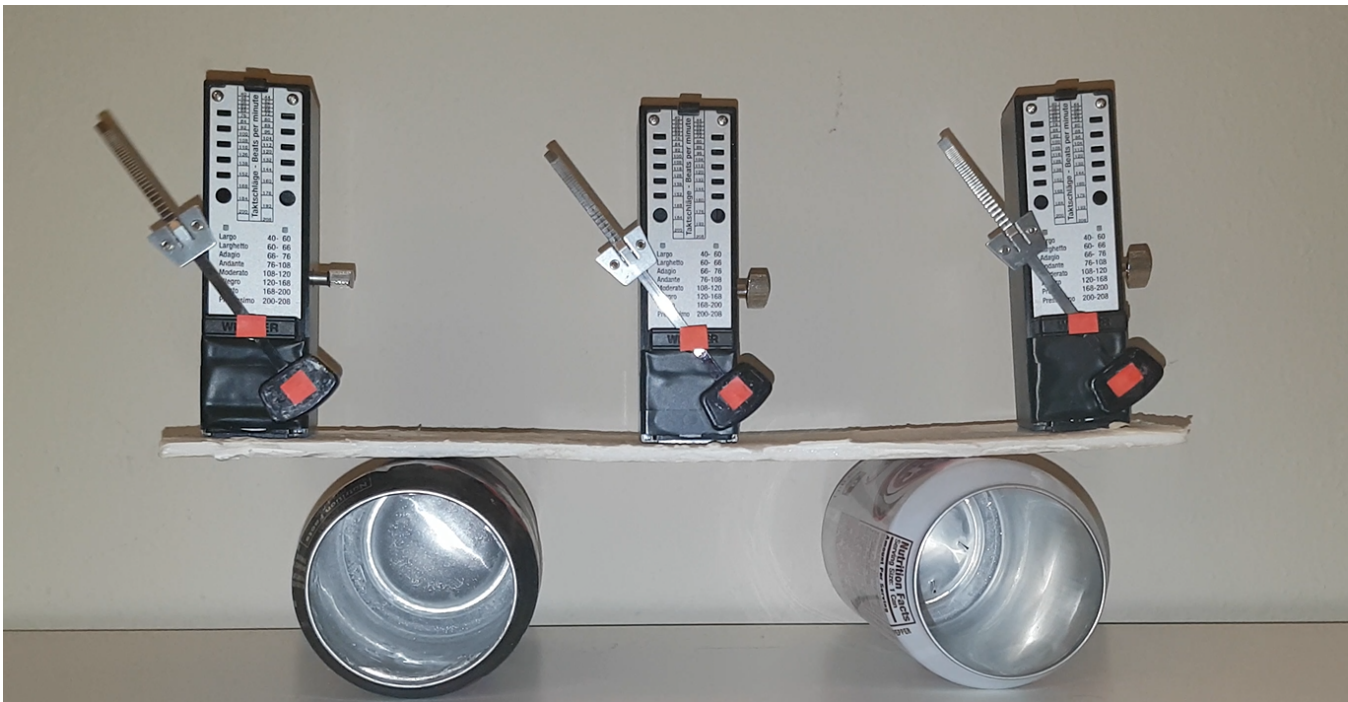


Fig.1: The experimental setup used for the project.

consisted of small tomato sauce cans, the masses of which were equal to 170g or 227g. Fig.1 provides an illustration of the setup.

Gathering and processing data corresponding to the oscillations of the metronomes was the most difficult part of our project. To do this, we decided to derive visual measurements of the metronomes' oscillations. Our measurement setup consists of a phone camera, a few red paper wafers and a computer. The resolution of the camera is 4K UHD, at 3840×2160 pixels and a frame rate of 30 Hz. The paper wafers that we used were colored with a red marker, and they were utilized in order to track the metronome bobs. We chose to place those wafers at the bottom end of the bobs. As the bottom end makes slower movements in the cartesian field, it is less noisy to track it and it appears less blurry in the JPEG images extracted from the video. In addition, the background was properly chosen so that it contains no elements whose color is close to the color of the paper wafers. This is important as we want to easily find the position of the wafers in the video frames.

Towards extracting the angles of the oscillating metronomes from the camera measurements, we used the software MATLAB, exploiting its integrated video and image processing tools. First, the video from the phone camera was imported into MATLAB in the form of an object. Then, a series of three dimensional matrices were extracted from the object, where each 3D matrix in the series corresponded to a video frame. Every 3D matrix consisted of three 2D matrices which provided the RGB code for each pixel of frame. Each of these 2D matrices was then divided into three parts, each of which corresponded spatially to a single metronome. Finally, a code was developed that searched each part of the frame matrices in order to find the position (in pixels) of the colored wafer on the metronome bob.

In the preprocessing phase of the trial, we estimated a range of RGB codes in which the color of the wafers could possibly lie. Hence, to find the position of the colored wafer, our MATLAB code was tasked with finding which pixels in each frame have an RGB color that lied in an appropriate range. Once the wafers were located, that point was marked as the required point. By locating the position (in pixels) of both the end of the bob and the pivot point of the metronomes, the metronome angle could be computed as $\phi_i = \arctan \delta y_p / \delta x_p$, where 90 degrees correspond to the nominal upward metronome position.

A brief presentation of the code is given below.

```

1 clear;
2 %% Read video
3 v = VideoReader('vid.mp4');
4 pos=zeros(v.NumFrames,1);
5 %% Set waffer's RGB range
6 range=[185 256; 60 130; 50 130];
7 %% Select which frames to analyze
8 rng1=6*30:14*30;
9 %% Scan the frames
10 th=zeros(length(rng1), n);
11 br=0;
12 for frn=rng1
13     frame = read(v,frn);
14     flag=zeros(n,1);
15     uppos=zeros(n,2);
16     downpos=zeros(n,2);
17     for i=round(size(frame,1)/2):4:size(frame,1)
18         for k=1:n
19             for j=(k-1)*floor(size(frame,2)/n)+1:4:k*floor(size(frame,2)/n)
20                 if frame(i,j,1)>=range(1,1) && frame(i,j,1)<=range(1,2) && frame(i,j,2)>=
21                     range(2,1) && frame(i,j,2)<=range(2,2) ...
22                         && frame(i,j,3)>=range(3,1) && frame(i,j,3)<=range(3,2)
23                     if flag(k)<5
24                         flag(k)=flag(k)+1;
25                     elseif flag(k)==5
26                         flag(k)=flag(k)+1;
27                         uppos(k,:)=[i j];
28                     elseif flag(k)<10 && norm(uppos(k,)-[i j])>100
29                         flag(k)=flag(k)+1;
30                     elseif flag(k)==10 && norm(uppos(k,)-[i j])>100
31                         flag(k)=flag(k)+1;
32                         downpos(k,:)=[i j];
33                         th(frn, k)=atan2(-(uppos(k,1)-downpos(k,1)), uppos(k,2)-downpos(k
34                             ,2))*180/pi;
35                     end
36                 end
37             end
38         end
39     th1=th;
40     th1=th1(rng1,:);
41     %% Plot figure of the angle
42     figure(1);
43     plot(rng1/v.FrameRate, th1, 'LineWidth', 2);
44     xlabel('t [s]');
45     xlim([rng1(1)/v.FrameRate rng1(end)/v.FrameRate]);

```

The “Scan the frames” part of the code can be explained as follows.

- Line 12: Analyze all frames between the 6th and the 14th second.
- Line 13: Select frame.
- Lines 14-16: Flags, indicating whether the upper and the lower wafer of each metronome has been found.
- Lines 17-19: Divide the frame in subsections, where only one metronome is located in each subsection.
- Line 20: Check whether a pixel of the subsection has an RGB code that falls in the range of the RGB code of the wafers.
- Lines 21-28: If line 20 is true, count that pixel. If a cluster of such pixels has been found, note their location and determine whether they correspond to the upper wafer or the lower wafer of the metronome.
- Lines 29-32: After both the upper and the lower wafer have been found, calculate the angle of the metronome using the arctangent.

III. THEORETICAL MODEL

We have found two distinct methods in the literature, which allow us to analyze theoretically the interconnected metronome system. The first method consists of a second-order nonlinear model, which can be obtained through the Euler-Lagrange equations [18], [19]. In particular, for all $i \in \{1, \dots, N\}$ metronomes, we have

$$\begin{aligned} \ddot{\phi}_i + b\dot{\phi}_i + \frac{g}{l} \sin \phi_i + \frac{1}{l} \ddot{x} \cos \phi_i + \bar{F}_i &= 0, \\ (M + Nm)\ddot{x} + B\dot{x} + Kx + ml \sum_{j=1}^N \sin \phi_j &= 0, \end{aligned} \quad (1)$$

where ϕ_i denotes the metronome bob's angle with the horizontal axis, x the position of the board, l the length of the bob and m , M the mass of the metronomes and the platform, respectively. Throughout the experiments, we will be varying the mass M of the platform, and study the effect of these variations on the ability of the metronomes to synchronize. We may easily notice that the system comprises $N + 1$ second order differential equations of motion, which correspond to the N metronomes as well as the moving base. This particular model is efficient in making the coupling mechanism in the physical level more clear. In addition, each metronome is affected by a friction term, namely $b\dot{\phi}_i$, which could eventually stop the oscillations had there not been a hand-wound spring to replenish the lost energy. The effect of this spring, called as ‘‘escapement’’ mechanism, is described as the force \bar{F}_i , and is typically modelled as a van der Pol term. The interconnection of the metronomes with the moving platform is also evident in the term $1/l\ddot{x} \cos \phi_i$, which appears in the metronome equations. Moreover, the friction that affects the oscillation of the platform is represented by the term $B\dot{x}$, where B is very close to zero as we used rigid soda cans to place the platform on. The platform is also affected by the motion of the metronomes. This coupling between the base and the metronomes is the basic mechanism that forces the metronomes to synchronize their phases.

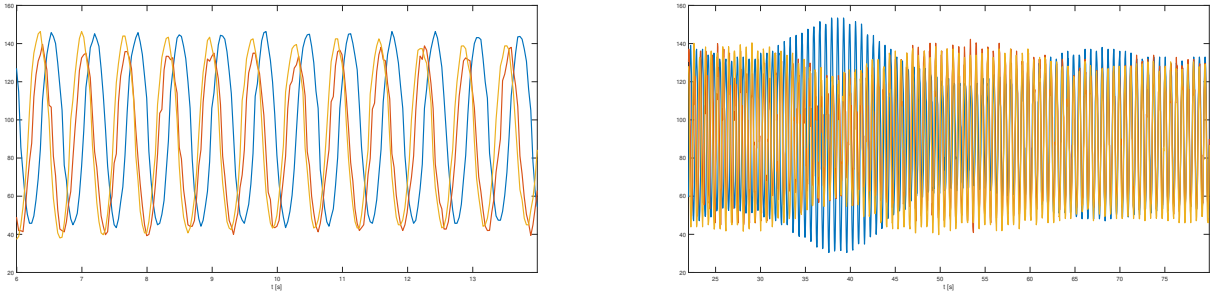
An other way to model the coupled metronome system is through the use of Kuramoto models, which are first order models shown to capture various synchronization phenomena. In their nominal form, the model of the Kuramoto oscillators is given by

$$\dot{\theta}_i = \omega_i + \frac{K}{N} \sum_{j=1}^N \sin(\theta_i - \theta_j), \quad \forall i \in \{1, \dots, N\}, \quad (2)$$

where θ_i, ω_i are the i -th metronomes phase and angular velocity, respectively. It should be highlighted that the phase of the oscillation θ_i is different than the angle ϕ_i . It has been proved that, through the use of averaging techniques [11], the behavior of the interconnected metronomes can actually be investigated with a Kuramoto model. The coupling parameter K depends on the system's mechanical properties, hence it will change as the mass of the platform varies.

IV. EXPERIMENTAL RESULTS

To begin, we conducted a simple 3-stage trial that showcased the phase synchronization/desynchronization of the 3 metronomes, and we also used this trial to test and debug the code for the visual measurements. The spring of the metronomes was wound by hand before the experiment. Initially, the metronomes were forced to oscillate and were placed on the foam/tin platform, which was located on a steady table. Due to the lack of coupling, no synchronization was observed at this stage. Then, the base with the metronomes were placed on the two soda cans, which induced an interconnection that forced the metronomes to synchronize. Finally, the metronomes and the base were moved off the soda cans and back to the table, which led to an eventual desynchronization of the oscillators' phases. Although the ideal model of the system would not indicate that desynchronization would take place after moving the metronomes off the soda cans, the disturbance induced in the system by the air and



(a) Metronome trajectories before coupling becomes active. (b) Metronome trajectories after coupling takes place: transience and eventual synchronization.

Fig.2: Synchronization of metronomes.

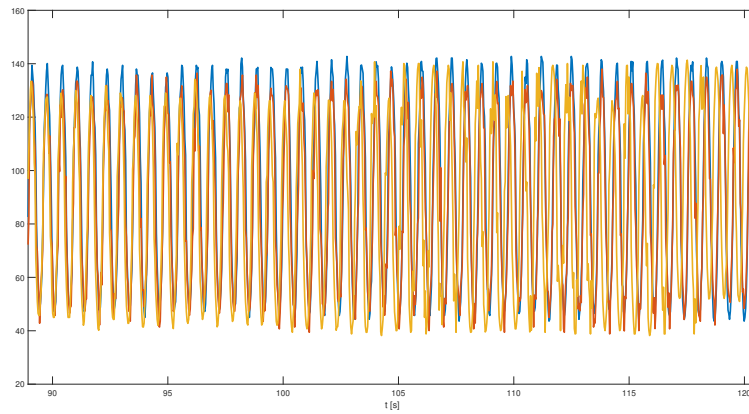


Fig. 3: Metronome trajectories after the decoupling takes place, and subsequent desynchronization.

the imperfections of the metronomes made the latter desynchronize. From Fig.2b, we can notice that once the coupling between the metronomes is activated, there is a transience period where the phases are not yet zero. After sufficient time has passed, the oscillators eventually synchronize their phases. This is not unexpected as, owing to the Kuramoto model of coupled oscillators, the states where the phase difference is a multiple of 2π is asymptotically stable. Fig.3 illustrates the third stage of the trial, where the metronomes are taken off the soda cans. Ideally, the Kuramoto model would predict that $\dot{\theta}_i = \omega_i$, meaning that the phases should continue to be synchronized. Nevertheless, the disturbances owing to the air and the imperfections of the metronomes cause the oscillators to slowly desynchronize at the end of that stage.

After the simple trial, we carried out a number of experimental runs, the aim of which was to showcase the effect of an increase in the mass of the platform on the synchronization of the metronomes. The most challenging part in this problem was decoupling the different parameters in each problem. Stopping the metronomes from oscillating, changing the platform's mass and restarting the experiment would mean that we would have no control over the initial conditions of the metronomes' angles, especially during the placement of the platform on top of the cans. Instead, we changed the mass of the platform once the metronomes were synchronized. Hence, whenever synchronization took place, we would add an extra single weight on the platform, which altered the coupling between the metronomes. Afterwards, to study the time to synchronization of the metronomes, we placed an obstacle on the path of one of the metronomes – specifically when $\phi_i = 90$, for a specific amount of time. As the metronomes' frequencies remain unchanged, the phase discrepancy generated during this period would be the same

in all runs of the system. Then, the metronomes were allowed to synchronize once again, and the time interval until synchronization was recorded. The data gathered are shown in the table that follows.

Synchronization time with different platform mass			
Foam platform		Tin platform	
Mass (kg)	Time (sec)	Mass (kg)	Time (sec)
0	8	0.200	10
0.170	13	0.654	31
0.340	43	1.108	66
0.567	50	1.562	600
0.794	80	2.016	∞

We can easily notice that, as the mass of the platform is increased, the time to synchronization is also increased. Looking at equation (2), we employ the results of [20], where the following Theorem is stated:

Theorem: The Kuramoto model given by (2) with $K > 0$, will synchronize to phase differences of an even multiple of 2π . The rate of approach to synchronization is no worse than $(2K/\pi N)\lambda_2(NI - \mathbf{1}_N \mathbf{1}_N^T/N)$, where I is the identity matrix of appropriate dimension, $\mathbf{1}_N$ a vector of ones and $\lambda_2(A)$ is the Fiedler eigenvalue of a matrix A .

As a result of this theorem, the linear dependence of the time to synchronization to the parameter K implies that an increase in the mass decreases K . Specifically, note that due to [11], the coupling parameter K can be computed as

$$K = \sqrt{\left(3\frac{\beta}{\mu}\right)^2 + \left(\frac{\beta}{\gamma}\right)^2 \left(\frac{\gamma}{2N}\right)},$$

where only the term $\beta = \left(\frac{m^2 r^2}{(M+2m)I}\right)$ is related to the board's mass. Hence, by increasing the mass of the platform, we are led to a decrease in β and, as a result, a decrease in K . In Fig. 4, we can notice the change of synchronization time as the mass changes.

Overall, we can conclude that the trend observed in our experimental results agrees with the monotonicity seen in the theoretical model of Kuramoto, suggesting that the time to synchronization increases as the mass of the moving platform increases. Nevertheless, as in all experiments, there are a number of discrepancies between our real-world setup and the ideal theoretical models given by both (1) and (2). For example, in our experiments:

- The mass of the moving platform was increased through the placement of sauce cans, which results in a non-uniform distribution of the overall total mass of the platform. As a result, it is not certain whether the total mass in the experiments could be represented by a single parameter M in the theoretical model (1).
- While friction is often parameterized by a linear damping term (as in (1)), it is generally highly nonlinear, especially if static friction is taken into account. As a result, the ideal models (1) and (2) could significantly differ from the “real” model of the system. Notice that this was the case in the tin platform - 2.016kg case, where the metronomes would never synchronize as static friction would not allow the soda cans to oscillate.
- The metronomes themselves cannot be entirely identical to one-another. It is safe to assume that they have slight differences, hence models like (1) and (2) will be different from the reality.

V. CONCLUSION

In this project, we studied the behavior of three coupled metronomes, emulating the experiments performed by Huygens, and characterized the effect of the mass of the moving platform on the time to synchronization. First, we created some software that is able to calculate the angle of the metronomes

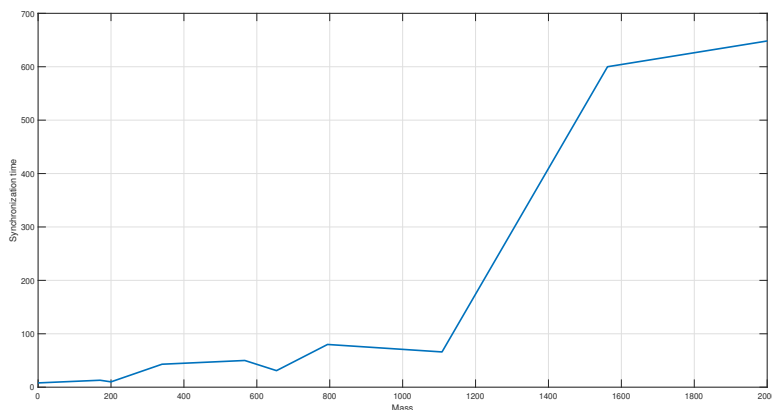


Fig. 4: Time to achieve synchronization as a function of the platform mass.

through visual measurements. In particular, our code divided the video into distinct parts at each frame, based on the platform’s position, and searches in those parts for the color-coded pointers in order to determine the position of the metronome bob. Hence, the metronomes’ angles are found trivially. After understanding the importance of the coupling induced by the platform, we considered a method that would allow us to find the time to synchronization from almost identical initial conditions as the platform mass was steadily increased. The theoretical results connecting the platform mass and the time to synchronization agree with our experimental results, though a more quantitative analysis would demand for a careful consideration and computation of the different factors affecting the time to synchronization. This line of research would experimentally support the connection between the abstract Kuramoto oscillator model and the Euler-Lagrange based second-order mechanical model of metronome synchronization.

REFERENCES

- [1] I. I. Blekhan, *Synchronization in science and technology*. ASME press, 1988.
- [2] A. R. Willms, P. M. Kitanov, and W. F. Langford, “Huygens’ clocks revisited,” *Royal Society Open Science*, vol. 4, no. 9, p. 170777, 2017.
- [3] S. H. Strogatz and I. Stewart, “Coupled oscillators and biological synchronization,” *Scientific American*, vol. 269, no. 6, pp. 102–109, 1993.
- [4] R. E. Mirollo and S. H. Strogatz, “Synchronization of pulse-coupled biological oscillators,” *SIAM Journal on Applied Mathematics*, vol. 50, no. 6, pp. 1645–1662, 1990.
- [5] S. H. Strogatz, “Norbert wiener’s brain waves,” in *Frontiers in mathematical biology*. Springer, 1994, pp. 122–138.
- [6] E. M. Izhikevich, “Weakly pulse-coupled oscillators, fm interactions, synchronization, and oscillatory associative memory,” *IEEE Transactions on Neural Networks*, vol. 10, no. 3, pp. 508–526, 1999.
- [7] A. Arenas, A. Díaz-Guilera, J. Kurths, Y. Moreno, and C. Zhou, “Synchronization in complex networks,” *Physics reports*, vol. 469, no. 3, pp. 93–153, 2008.
- [8] A. Pluchino, V. Latora, and A. Rapisarda, “Changing opinions in a changing world: A new perspective in sociophysics,” *International Journal of Modern Physics C*, vol. 16, no. 04, pp. 515–531, 2005.
- [9] T. Miyano and T. Tsutsui, “Data synchronization in a network of coupled phase oscillators,” *Physical review letters*, vol. 98, no. 2, p. 024102, 2007.
- [10] G. Filatrella, A. H. Nielsen, and N. F. Pedersen, “Analysis of a power grid using a kuramoto-like model,” *The European Physical Journal B*, vol. 61, no. 4, pp. 485–491, 2008.
- [11] J. Pantaleone, “Synchronization of metronomes,” *American Journal of Physics*, vol. 70, no. 10, pp. 992–1000, 2002.
- [12] J. A. Acebrón, L. L. Bonilla, C. J. P. Vicente, F. Ritort, and R. Spigler, “The kuramoto model: A simple paradigm for synchronization phenomena,” *Reviews of modern physics*, vol. 77, no. 1, p. 137, 2005.
- [13] G. H. Goldsztein, A. N. Nadeau, and S. H. Strogatz, “Antiphase versus in-phase synchronization of coupled pendulum clocks and metronomes,” *arXiv preprint arXiv:2008.02947*, 2020.
- [14] E. A. Martens, S. Thutupalli, A. Fourrière, and O. Hallatschek, “Chimera states in mechanical oscillator networks,” *Proceedings of the National Academy of Sciences*, vol. 110, no. 26, pp. 10 563–10 567, 2013.
- [15] M. Francke, A. Pogromsky, and H. Nijmeijer, “Huygens’ clocks: ‘sympathy’ and resonance,” *International Journal of Control*, vol. 93, no. 2, pp. 274–281, 2020.

- [16] J. Jia, Z. Song, W. Liu, J. Kurths, and J. Xiao, "Experimental study of the triplet synchronization of coupled nonidentical mechanical metronomes," *Scientific reports*, vol. 5, no. 1, pp. 1–12, 2015.
- [17] Y. Wu, N. Wang, L. Li, and J. Xiao, "Anti-phase synchronization of two coupled mechanical metronomes," *Chaos: An Interdisciplinary Journal of Nonlinear Science*, vol. 22, no. 2, p. 023146, 2012.
- [18] M. Bennett, M. F. Schatz, H. Rockwood, and K. Wiesenfeld, "Huygens's clocks," *Proceedings of the Royal Society of London. Series A: Mathematical, Physical and Engineering Sciences*, vol. 458, no. 2019, pp. 563–579, 2002.
- [19] M. Kapitaniak, K. Czolczynski, P. Perlikowski, A. Stefanski, and T. Kapitaniak, "Synchronization of clocks," *Physics Reports*, vol. 517, no. 1-2, pp. 1–69, 2012.
- [20] A. Jadbabaie, N. Motee, and M. Barahona, "On the stability of the kuramoto model of coupled nonlinear oscillators," in *Proceedings of the 2004 American Control Conference*, vol. 5. IEEE, 2004, pp. 4296–4301.